Supplementary Information

A Highly Selective "Turn-on" Water-soluble Fluorescent Sensor for Gallium Ion Detection

Pengfei Wang,[a] Fanda Meng,[b] Hao Su,[a] Lijie Liu,[a] Maroof Ahmad Khan,[a] Hui Li*[a]

[a] Key Laboratory of Cluster Science of Ministry of Education, School of Chemistry and Chemical Engineering, Beijing Institute of Technology, Beijing 100081, P. R. China.

[b] School of Basic Medicine, Shandong First Medical University & Shandong Academy of Medical Sciences, Jinan, 250062, P. R. China.

*** Correspondence:**

Hui Li

E-mail: lihui@bit.edu.cn

Table of Contents:

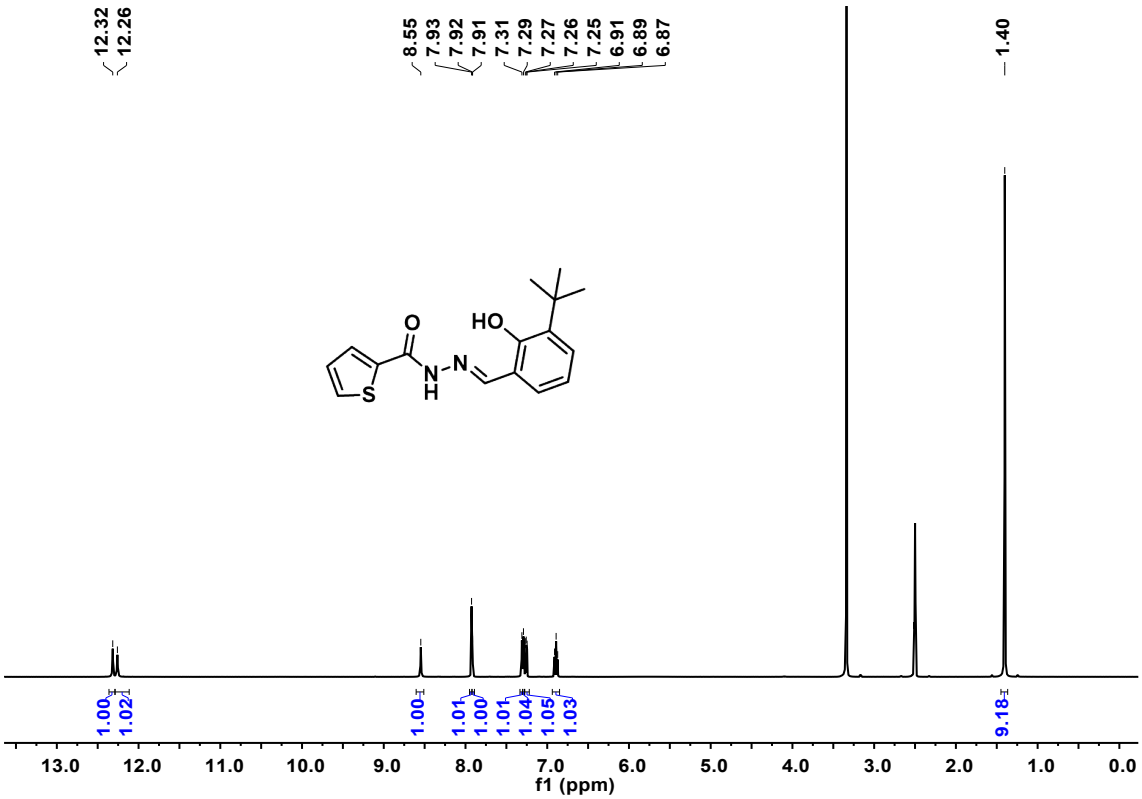

Figure S1. ^{1}H NMR (400 MHz, DMSO-d_6) spectrum of **1**.

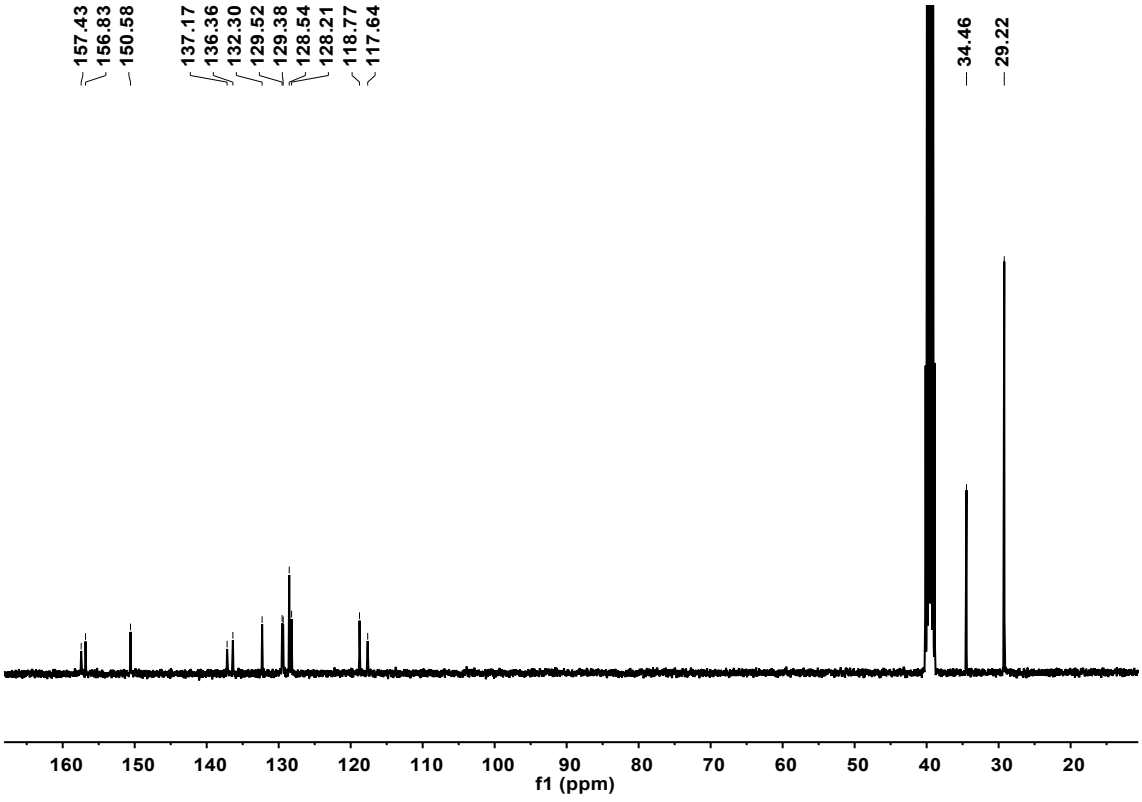

Figure S2. ^{13}C NMR (176 MHz, DMSO-d_6) spectrum of **1**.

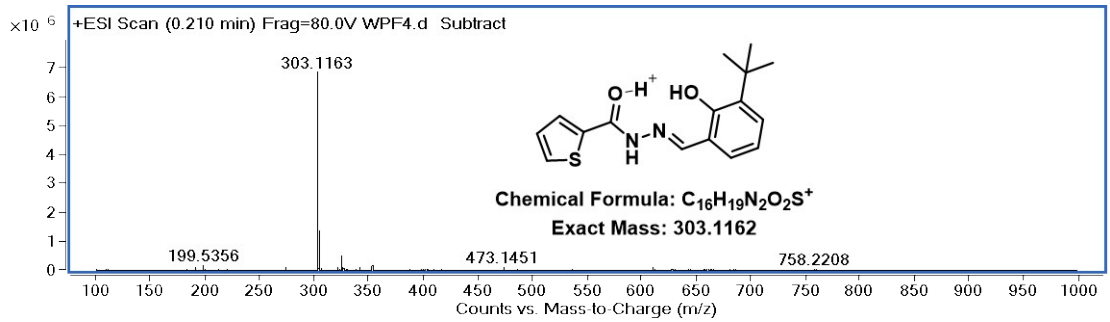

Figure S3. Positive-ion ESI-mass spectrum of **1**.

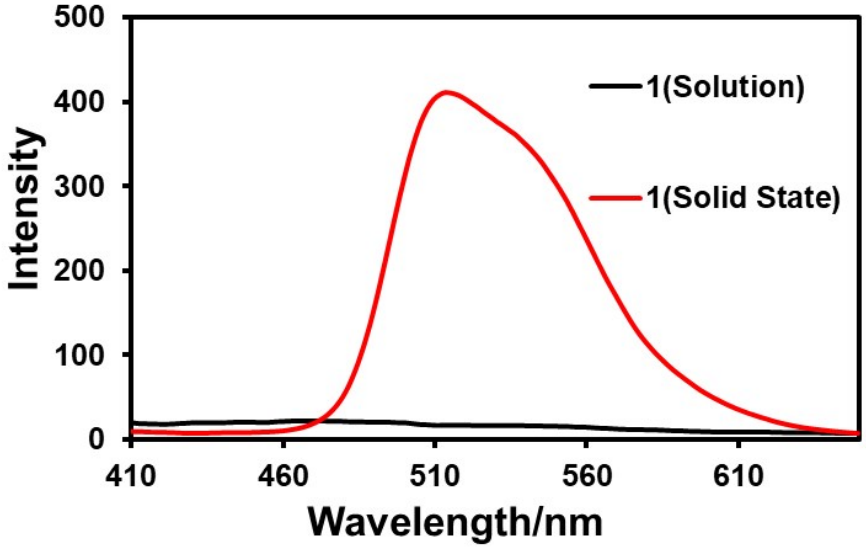

Figure S4. Solution and Solid State Fluorescence spectrum of **1.**

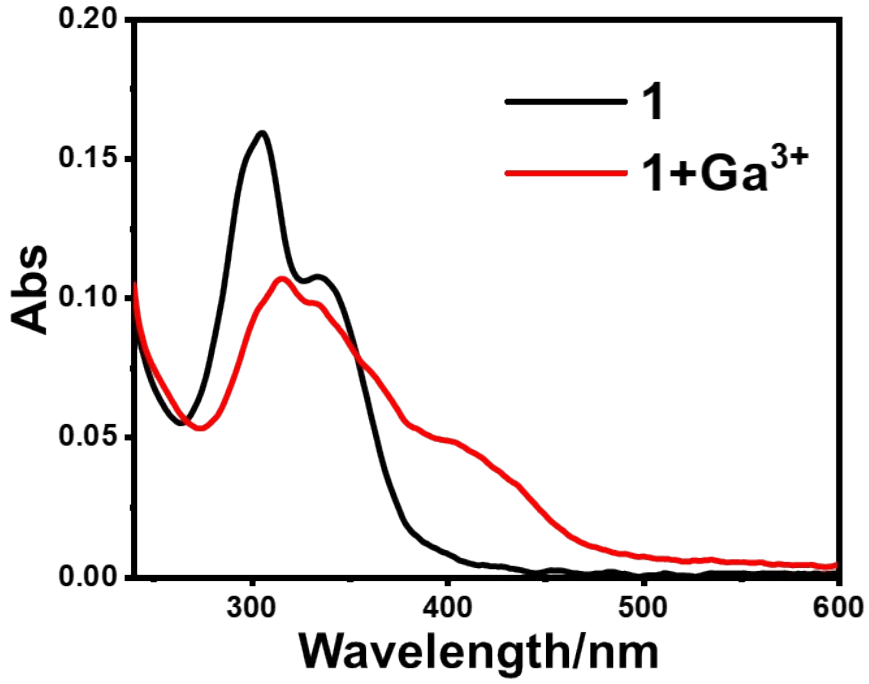

Figure S5. Absorption spectrum of **1** (10 μM) and **1-Ga**$^{3+}$(10 μM) in 0.1% DMSO/bis-tris buffer solution.

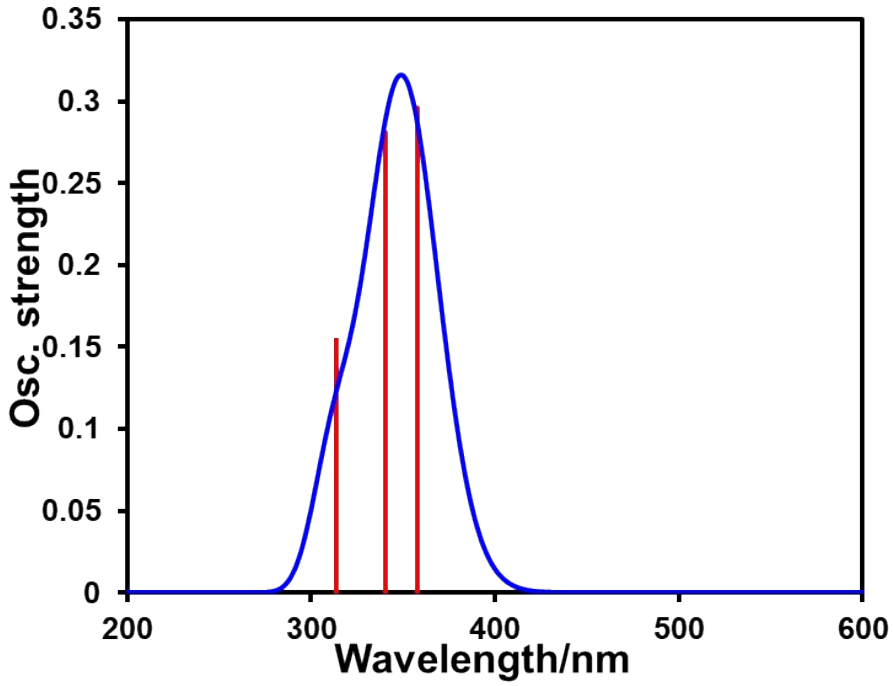

Figure S6. Theoretical calculated UV-vis absorption spectrum of **1**.

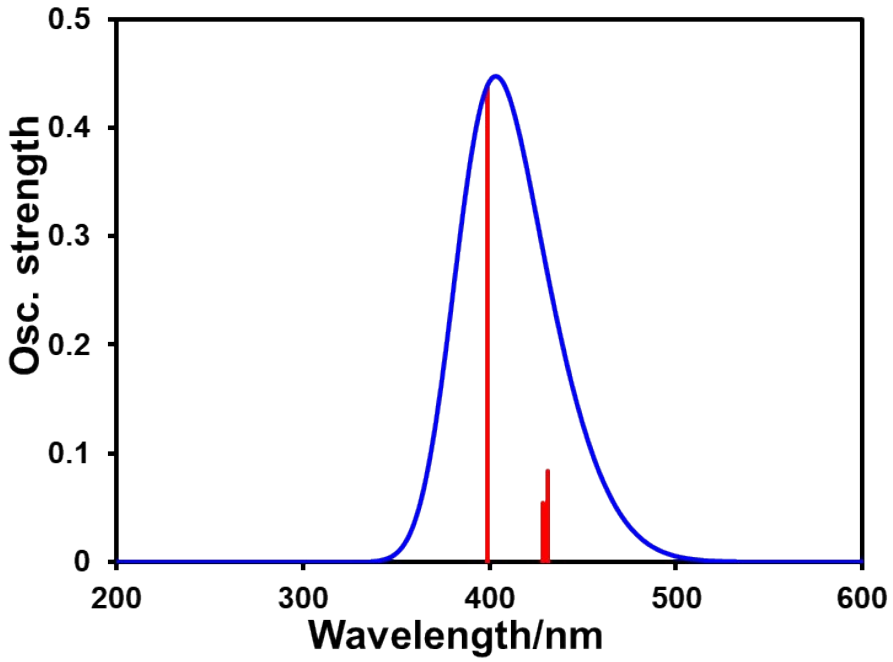

Figure S7. Theoretical calculated UV-vis absorption spectrum of **1-Ga**$^{3+}$.

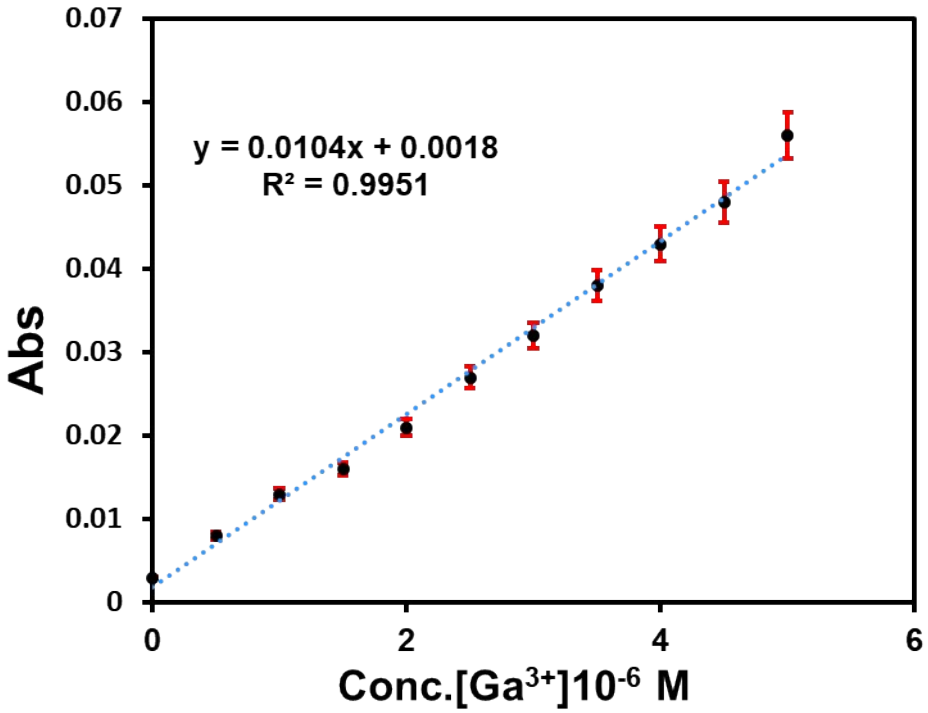

Figure S8. The calibration curve of **1** versus Ga^{3+} concentrations.

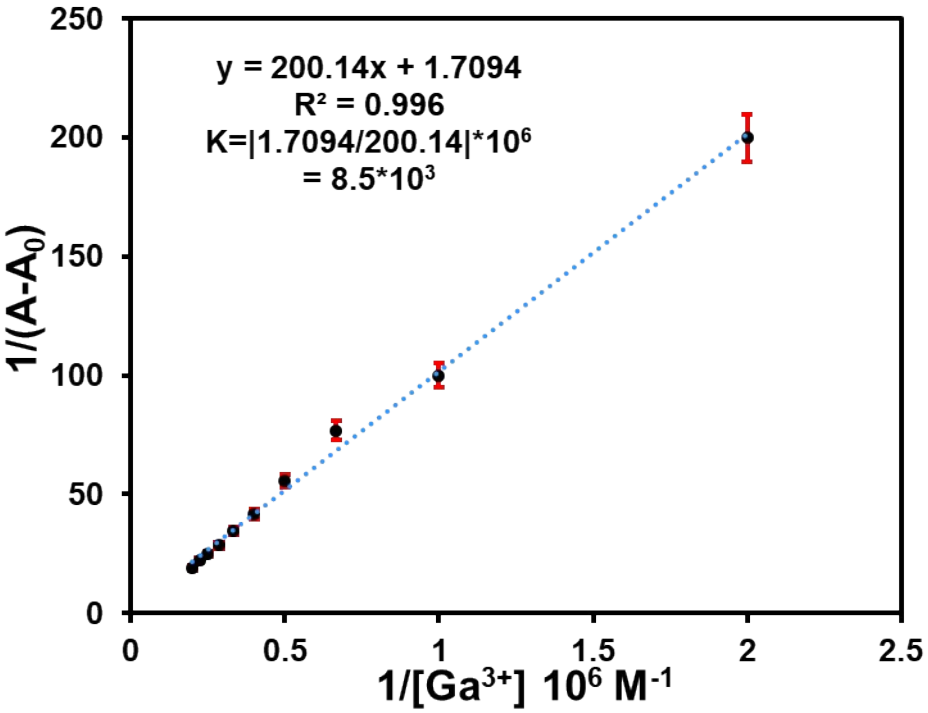

Figure S9. Benesi-Hildebrand plot of **1** and Ga^{3+}.

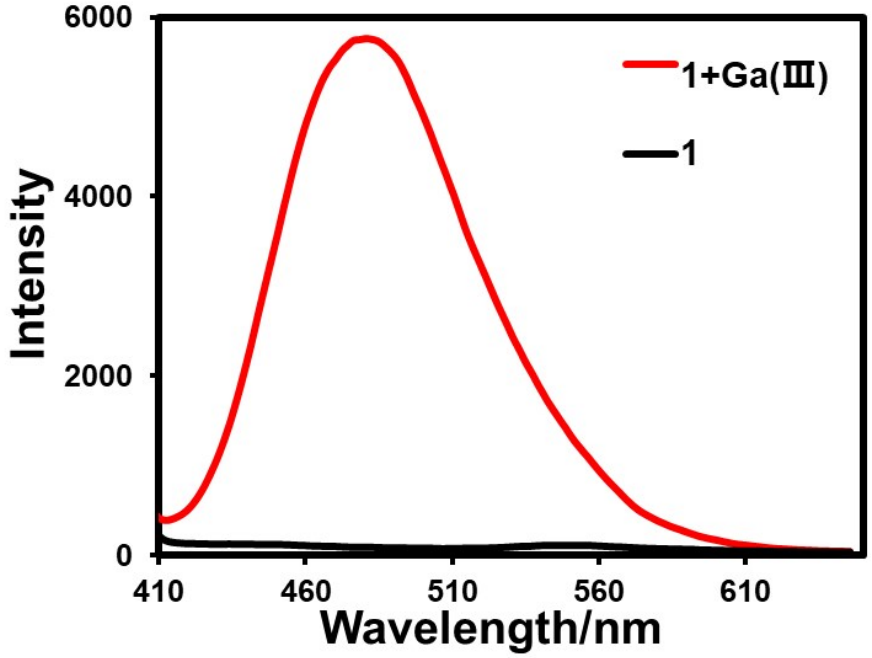

Figure S10. Fluorescence spectrum of **1** (1 μM) and **1-Ga**$^{3+}$(1 μM) in 0.1% DMSO/bis-tris buffer solution.

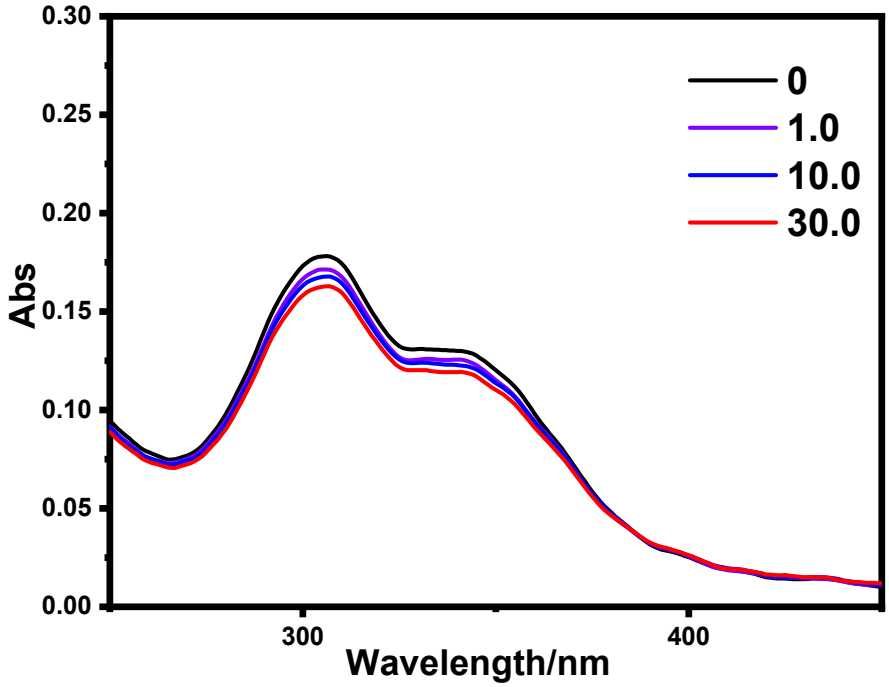

Figure S11. Absorption spectra of **1** (10 μM) upon the addition of Al^{3+}(0- 30 eq.) in 0.1% DMSO/bis-tris buffer solution;

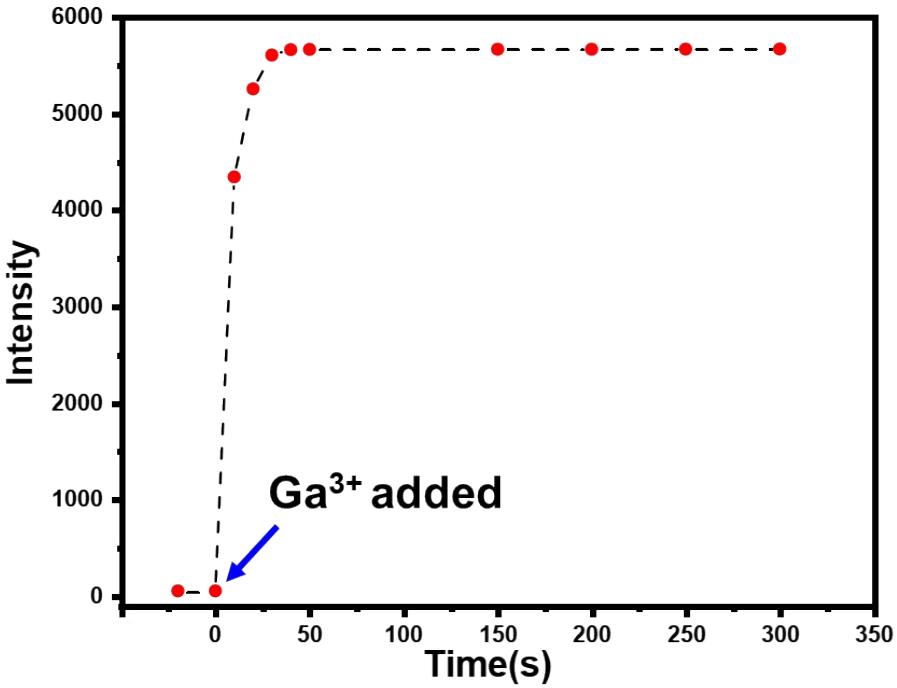

Figure S12. Time-dependent fluorescence response of probe **1** in the presence of Ga^{3+} ions.

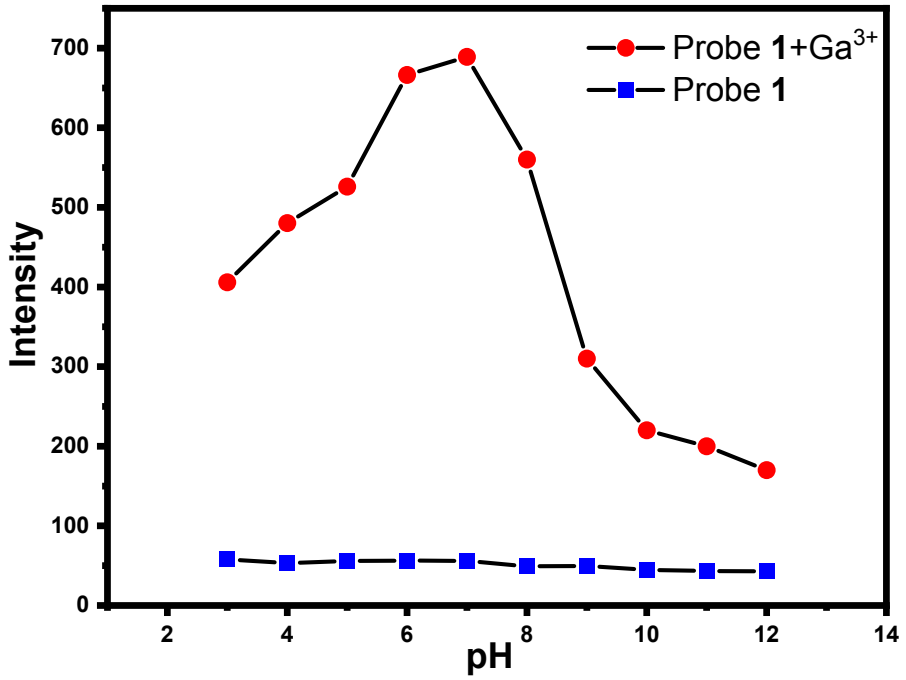

Figure S13. Effect of pH on the fluorescence intensities of **1** and the **1-**Ga^{3+} complex.

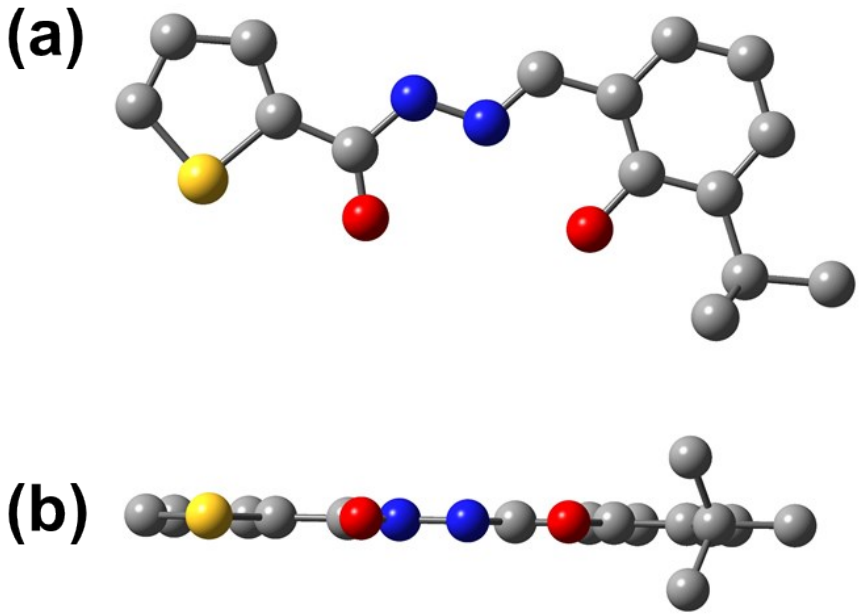

Figure S14. Up view (a) and side view (b) of the optimized molecular structure of sensor **1**.

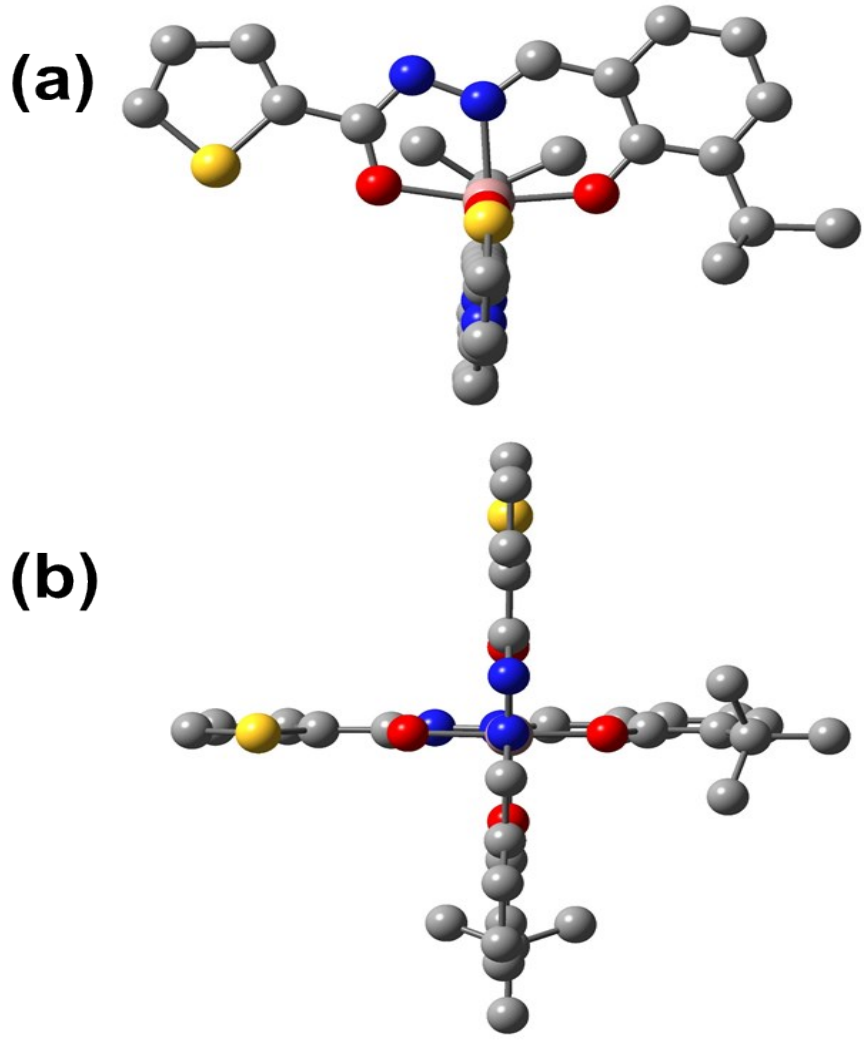

Figure S15. Up view (a) and side view (b) of the optimized molecular structure of **1-Ga**$^{3+}$.

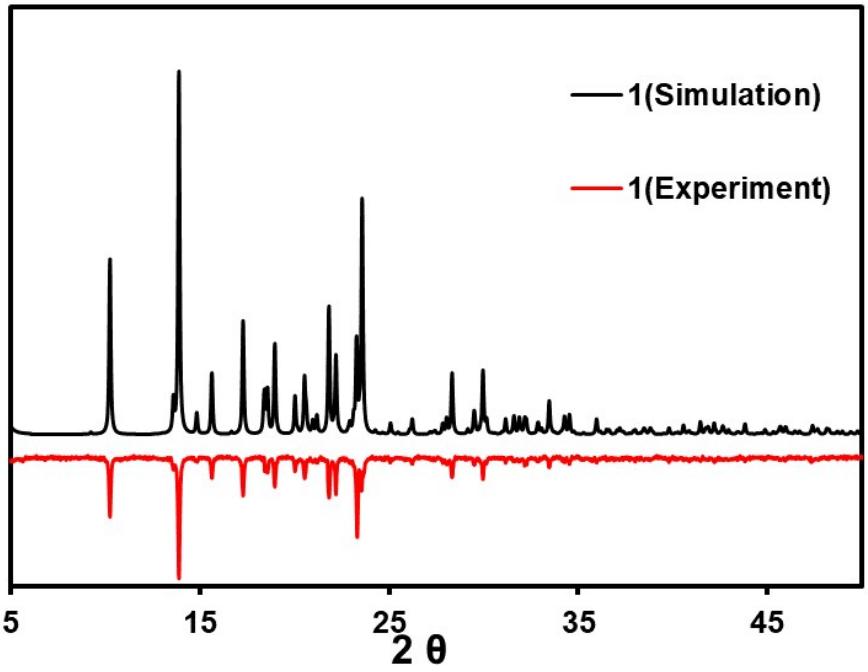

Figure S16. PXRD patterns of **1.**

Table S1. Bond Lengths for **1**.

Atom	Atom	Length/Å	Atom	Atom	Length/Å
S1	C1	1.649(5)	C6	C7	1.441(5)
S1	C4	1.683(4)	C7	C8	1.390(5)
O1	C5	1.223(4)	C7	C11	1.404(5)
O2	C11	1.358(4)	C8	C9	1.374(6)
N1	N2	1.369(4)	C9	C10	1.379(6)
N1	C5	1.354(4)	C10	C12	1.381(5)
N2	C6	1.282(4)	C11	C12	1.411(5)
C1	C2	1.338(6)	C12	C13	1.532(6)
C2	C3	1.426(6)	C13	C14	1.537(6)
C3	C4	1.458(5)	C13	C15	1.544(5)
C4	C5	1.475(5)	C13	C16	1.532(5)

Table S2 Bond Angles for **1**.

Atom	Atom	Atom	Angle/°	Atom	Atom	Atom	Angle/°
C1	S1	C4	92.3(2)	C9	C8	C7	120.3(4)
C5	N1	N2	119.5(3)	C8	C9	C10	119.5(4)
C6	N2	N1	117.0(3)	C9	C10	C12	123.6(4)
C2	C1	S1	113.9(3)	O2	C11	C7	120.0(3)
C1	C2	C3	114.9(4)	O2	C11	C12	118.3(3)

Atom	Atom	Atom	Angle/°	Atom	Atom	Atom	Angle/°
C2	C3	C4	106.2(3)	C7	C11	C12	121.7(3)
C3	C4	S1	112.6(2)	C10	C12	C11	116.0(4)
C3	C4	C5	128.6(3)	C10	C12	C13	122.3(3)
C5	C4	S1	118.7(3)	C11	C12	C13	121.8(3)
O1	C5	N1	123.2(3)	C12	C13	C14	111.0(3)
O1	C5	C4	122.3(3)	C12	C13	C15	109.7(3)
N1	C5	C4	114.5(3)	C12	C13	C16	111.8(3)
N2	C6	C7	122.1(3)	C14	C13	C15	109.5(4)
C8	C7	C6	118.5(3)	C16	C13	C14	107.4(3)
C8	C7	C11	119.0(3)	C16	C13	C15	107.4(3)
C11	C7	C6	122.5(3)				

Table S3. Performance comparison of recently published sensors.

Ref.	Crystal	Media	Detection Ions	LOD(M)	Applications
[1]	NA	DMSO/MeOH	Ga^{3+}, Al^{3+}, and In^{3+}	1.4×10^{-5}	NA
[2]	NA	EtOH/H_2O (98:2)	Hcy and Ga^{3+}	2.4×10^{-6}	NA
[3]	NA	DMSO/H_2O/ EtOH	Al^{3+}, and Ga^{3+}	5×10^{-8}	NA
[4]	NA	MeOH	Al^{3+}, and Ga^{3+}	1×10^{-7}	NA
[5]	NA	DMSO/H_2O (5:1)	Ga^{3+}, Al^{3+}, and In^{3+}	5.4×10^{-8}	Bioimaging
[6]	NA	MeCN	Ga^{3+}	5.5×10^{-7}	Bioimaging
This work	YES	H_2O	Ga^{3+}	5.8×10^{-8}	Test strips Water Samples

Table S4. Primary orbitals which contribute to the calculated transitions of **1** (iso = 0.03).

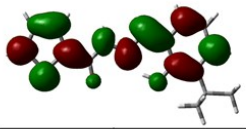		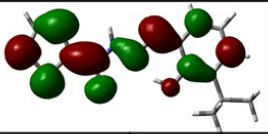		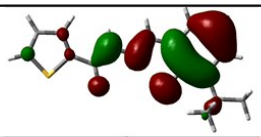		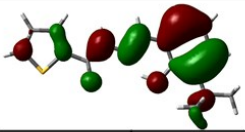	
LUMO+1	**-0.96 eV**	**LUMO**	**-1.78 eV**	**HOMO**	**-5.69 eV**	**HOMO-1**	**-6.24 eV**

Table S5. Primary orbitals which contribute to the calculated transitions of **1-Ga^{3+}** (iso = 0.03).

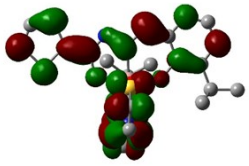		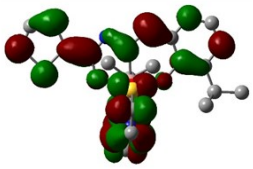		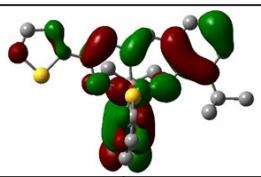		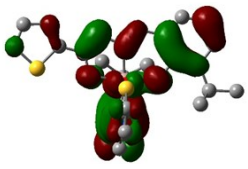	
LUMO+1	1.24 eV	LUMO	1.10 eV	HOMO	-2.26 eV	HOMO-1	-2.29 eV

Table S6. TD-DFT calculated electronic transition configurations for **1 and 1-Ga^{3+}** along with their corresponding excitation energies and oscillator strengths.

	Spin State	Transition Configuration	Excitation Energy (nm, eV)	Oscillator Strength
1	S1	HOMO → LUMO (98%)	358.0 (3.46)	0.2956
	S2	HOMO-1 → LUMO (92%)	340.6 (3.64)	0.2812
	S3	HOMO → LUMO+1 (86%)	313.6 (4.95)	0.1538
1+Ga^{3+}	S1	HOMO-1 → LUMO+1 (10%)	431.4 (2.87)	0.0837
		HOMO → LUMO (89%)		
	S2	HOMO-1 → LUMO (83%)	428.3 (2.89)	0.0544
		HOMO → LUMO+1 (16%)		
	S3	HOMO-1 → LUMO (16%)	398.9 (3.11)	0.4384
		HOMO → LUMO+1 (82%)		

Reference

[1] H. J. Jang, J. H. Kang, D. Yun and C. Kim, *Photochem. Photobiol. Sci.*, **2018**, 17, 1247-1255;

[2] Y. W. Wang, S. B. Liu, W. J. Ling, Y. Peng, *Chem. Commun.*, **2016**, 52, 827-830;

[3] J. Kimura, H. Yamada, H Ogura, T. Yajima and T. Fukushima, *Anal. Chim. Acta*, **2009**, 635, 207-213;

[4] J. Y. Noh, S. Kim, I. H. Hwang, G. Y. Lee, J. S. Kang, H. Kim, J. Min, S. Park, C. Kim and J. Kim, *Dyes Pigm.*, **2013**, 99, 1016-1021;

[5] X. He, W. Xiong, C. Xu, J. Fan, Y. Qian, J. Wen and J. Shen, *Dyes Pigm.*, **2020**, 174, 108059;

[6] L. Xiao, S. Sun, Z. Pei, Y. Pei, Y. Pang and Y. Xu, *Biosens. Bioelectron.*, **2015**, 65, 166-170.